

# GALAXY-GALAXY LENSING AS A PROBE OF GALAXY DARK MATTER HALOS

M. LIMOUSIN<sup>1</sup>, J.-P. KNEIB<sup>2</sup> & P. NATARAJAN<sup>3</sup>

<sup>1</sup> *Dark Cosmology Centre, Niels Bohr Institute, Juliane Maries Vej 30, 2100 Copenhagen, Denmark*

<sup>2</sup> *OAMP, Laboratoire d'Astrophysique de Marseille, Traverse du siphon, 13012 Marseille, France*

<sup>3</sup> *Department of Astronomy, Yale University, 260 Whitney Avenue, New Haven, CT 06511, USA*

Gravitational lensing has now become a popular tool to measure the mass distribution of structures in the Universe on various scales. Here we focus on the study of galaxy's scale dark matter halos with galaxy-galaxy lensing techniques: observing the shapes of distant background galaxies which have been lensed by foreground galaxies allows us to map the mass distribution of the foreground galaxies. The lensing effect is small compared to the intrinsic ellipticity distribution of galaxies, thus a statistical approach is needed to derive some constraints on an average lens population. An advantage of this method is that it provides a probe of the gravitational potential of the halos of galaxies out to very large radii, where few classical methods are viable, since dynamical and hydrodynamical tracers of the potential cannot be found at this radii. We will begin by reviewing the detections of galaxy-galaxy lensing obtained so far. Next we will present a maximum likelihood analysis of simulated data we performed to evaluate the accuracy and robustness of constraints that can be obtained on galaxy halo properties. Then we will apply this method to study the properties of galaxies which stand in massive cluster lenses at  $z \sim 0.2$ . The main result of this work is to find dark matter halos of cluster galaxies to be significantly more compact compared to dark matter halos around field galaxies of equivalent luminosity, in agreement with early galaxy-galaxy lensing studies and with theoretical expectations, in particular with the tidal stripping scenario. We thus provide a strong confirmation of tidal truncation from a homogeneous sample of galaxy clusters. Moreover, it is the first time that cluster galaxies are probed successfully using galaxy-galaxy lensing techniques from ground based data.

This contribution is a summary of two galaxy-galaxy lensing papers: Limousin et al., 2005<sup>25</sup>, hereafter Paper I exposes a theoretical analysis of galaxy-galaxy lensing, and Limousin et al., 2006<sup>26</sup>, hereafter Paper II exposes the application of the method tested extensively in Paper I on a sample of homogeneous massive galaxy cluster at  $z \sim 0.2$ .

## 1 Galaxy-Galaxy Lensing

The main goal of galaxy-galaxy lensing studies is to obtain constraints on the physical parameters that characterise the dark matter halos of galaxies. A dark matter halo can be described by two parameters: in this work we will mainly use  $\sigma_0$ , the central velocity dispersion, which is related to the depth of the potential well, and  $r_{\text{cut}}$ , the cut off radius, which is related to the spatial extension of the halo since it defines a change in the slope of the three dimensional mass density profile: below  $r_{\text{cut}}$ , the profile falls with radius (see Paper I for a detailed description of galaxy dark matter halo modeling).

The first statistically significant detection of galaxy-galaxy lensing is the work by Brainerd,

Blandford & Smail, 1996<sup>7</sup>, hereafter BBS. They used deep ground-based imaging data ( $\simeq 72$  sq. arcminute) to investigate the orientation of 511 faint background galaxies relative to 439 brighter foreground field galaxies. They claimed a detection of galaxy-galaxy lensing on angular scales between  $5''$  and  $35''$  and derived limits on the characteristic parameters of the dark matter halos of  $L^*$  field galaxies :  $\sigma_0 = 155 \pm 56 \text{ km s}^{-1}$  and  $r_{\text{cut}} > 100h^{-1} \text{ kpc}$ . Since BBS, there have been 12 independent detections of galaxy-galaxy lensing by field galaxies: Griffiths et al., 1996<sup>18</sup>; Dell’Antonio & Tyson, 1996<sup>13</sup>; Hudson et al., 1998<sup>21</sup>; Ebbels et al., 1998<sup>14</sup>; Fisher et al., 2000<sup>15</sup>; Jansen, 2000<sup>22</sup>; McKay et al., 2001<sup>27</sup>; Smith et al., 2001<sup>34</sup>; Wilson et al., 2001<sup>35</sup>; Hoekstra et al., 2002<sup>19</sup>; Kleinheinrich, 2003<sup>24</sup>; Hoekstra et al., 2004<sup>20</sup>. Galaxy-galaxy lensing has also been used successfully to map substructure in massive lensing clusters (Natarajan et al., 1998<sup>28</sup>, 2002a<sup>29</sup>, 2002b<sup>30</sup>; Geiger & Schneider, 1998<sup>16</sup>). Analyses on cluster galaxies all used HST data for their investigations, and most of them included strong constraints from observation of multiple images systems.

Fig. 1 illustrates the results of the different detections in term of constraints in the  $(\sigma_0, r_{\text{cut}})$  plane. Before comparing these results, one has to keep in mind that there is considerable variation between data sets and the analysis techniques used by the various authors. The imaging quality, size of the field, the dichotomy between lenses and sources differs significantly amongst these investigations. Moreover, the data are a heterogeneous mix of deep images which were acquired for purposes other than galaxy-galaxy lensing studies. Despite these differences, the implications of these studies for the physical characteristics of the halos of field galaxies are all broadly consistent with one another, and the results on field galaxies are in good agreement with studies based on satellite dynamics (see *e.g.* Prada et al., 2003<sup>32</sup>).

From Fig. 1, a clear trend can be seen: dark matter halos in cluster are significantly more compact compared to halos around field galaxies of equivalent luminosity. This is a landmark observational result provided by galaxy-galaxy lensing studies that was expected from theoretical considerations and numerical simulations: when clustering, galaxies do experience strong tidal stripping from the cluster potential, and they loose part of their dark matter halo, feeding the global cluster dark matter halo itself.

We can say that the last ten years since the first detection of galaxy-galaxy lensing have been ‘experimental’ in the sense that these early studies have demonstrated convincingly that galaxy-galaxy lensing, though challenging to detect, is a viable technique by which the dark matter distribution on scales of individual galaxies can be investigated. Now that the technique has been proved, galaxy-galaxy lensing appears as very promising to get interesting statistical constraints on galaxy physics (halo parameter determination, mass measurements, M/L ratio and evolution with redshift and environment; deviation from spherical symmetry for dark matter halos; morphological dependence of the halo potential; scaling of the total galaxy mass with luminosity; truncation of dark matter halos during the infall of galaxies into cluster; nature of dark matter - see Paper II for more details).

## 2 Simulating Galaxy-Galaxy Lensing

We first introduce some mass models to describe galaxies, and expose the simulation procedure and the methodology. Then we present some results. More details can be found in Paper I.

### 2.1 Modeling the mass distribution of galaxies

Two different mass models are used to model galaxy dark matter halos: (i) the two components Pseudo-Isothermal Elliptical Mass Distribution (PIEMD, Kassiola & Kovner, 1993<sup>23</sup>), which is a more physically motivated mass profile than the isothermal sphere profile (SIS) but sharing the same slope at intermediate radius and (ii) the ‘universal’ NFW profile (Navarro, Frenk &

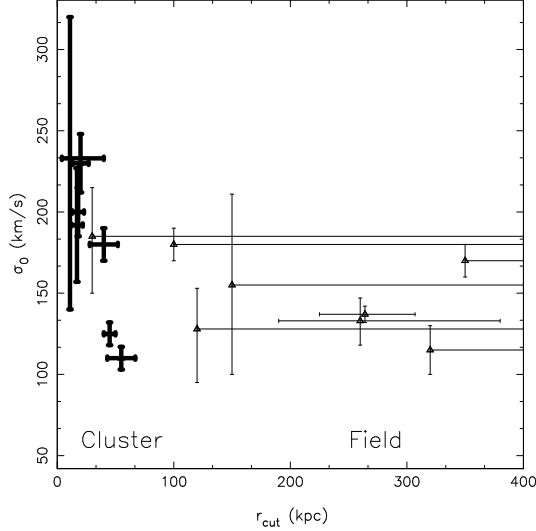


Figure 1: Comparison between galaxy-galaxy lensing results on cluster galaxies (black) and galaxy-galaxy lensing results on field galaxies (grey): cluster galaxies appear to be significantly more compact than field galaxies

White, 1996<sup>31</sup>).

### PIEMD profile:

The density distribution for this model is given by:

$$\rho(r) = \frac{\rho_0}{(1 + r^2/r_{\text{core}}^2)(1 + r^2/r_{\text{cut}}^2)} \quad (1)$$

with the core radius  $r_{\text{core}}$  of the order of  $0.1''$ , and a truncation radius  $r_{\text{cut}}$ . In the centre,  $\rho \sim \rho_0/(1 + r^2/r_{\text{core}}^2)$  which describes a core with central density  $\rho_0$ . The transition region ( $r_{\text{core}} < r < r_{\text{cut}}$ ) is isothermal, with  $\rho \sim r^{-2}$ . In the outer parts, the density falls off as  $\rho \sim r^{-4}$ , as is usually required for models of elliptical galaxies. This mass distribution is described by a central velocity dispersion  $\sigma_0$  related to  $\rho_0$ . It is easy to show that for a vanishing core radius, the surface mass density profile obtained above becomes identical to the surface mass profile used by BBS for modeling galaxy-galaxy lensing. Since many authors are using the same mass profile in their galaxy-galaxy lensing studies, it allows easy comparison of our results. It should be noted that a dark matter halo parametrised by  $r_{\text{cut}}$  still have a significant amount of mass below  $r_{\text{cut}}$ : the mass profile become steeper, but about half of the mass is contained below  $r_{\text{cut}}$ . Thus  $r_{\text{cut}}$  can be considered as a half mass radius.

### NFW profile:

The NFW density profile provides a good fit to the halos that form in N-body simulations of collisionless dark matter, over 9 orders of magnitudes in mass, from the scale of globular clusters to that of massive galaxy clusters. The density distribution of the NFW profile is given by:

$$\rho(r) = \frac{\rho_s}{(r/r_s)(1 + r/r_s)^2} \quad (2)$$

where  $r_s$  is a characteristic radius that defines a change in the slope of the density profile. This mass distribution is described by a characteristic velocity dispersion  $\sigma_s$  related to  $\rho_s$ . It can be also parametrised in terms of  $M_{200}$ , which is the mass contained in a radius  $r_{200}$  where the criterion  $\bar{\rho} = 200\rho_{\text{crit}}$  holds, and  $c = r_{200}/r_s$ , the concentration parameter.

## 2.2 Simulating images

We describe foreground lenses by a mass profile with known input parameters, scaled as a function of luminosity. We put the individual lenses constituting a cluster at a redshift of 0.2, and model it as a superposition of a large-scale smooth cluster component and a few clumps associated with individual galaxies. The background source population is distributed as follows: they are allocated random positions, number counts are generated in consonance with galaxy counts typical for a 2 hour integration time in the R-band; the magnitudes are assigned by drawing the number count observed with the CFHT and the mean redshift per magnitude bin is derived from the HDF prescription; the shapes are assigned by drawing the ellipticity from a Gaussian distribution similar to the observed CFHT ellipticity distribution. Typical density is 17 per arcmin<sup>2</sup>. We then ray-trace the lensing configuration using the publicly available LENSTOOL<sup>a</sup> software to get a catalogue of images that we analyse as describe in next subsection.

## 2.3 Methodology

The details of the method have been given in Paper I. Here we just give a brief outline of the method. Two methods are used in galaxy-galaxy lensing analysis. The most direct method consists of obtaining an average shear field by simply binning up the shear in radial bins from the centre of the lens outwards, and stacking many individual galaxy shear profiles to obtain a signal and to constrain an average galaxy halo population. Such a method is possible when studying isolated field galaxies, since it makes the assumption that we are able to isolate a lens in order to study it. However, this assumptions is a very unlikely one, and galaxy-galaxy lensing is fundamentally a multiple deflection problem, even when studying field galaxies. This was first pointed out by BBS in their early work, who found that more than 50% of their source galaxies should have been lensed by two or more foreground galaxies: the closest lens on the sky to any given source was not necessarily the only lens, and neither the strongest lens. It has become clear that it is almost never a unique lens that is responsible for the detected lensing signal and that there are indeed no clean lines of sight. Consequently, the problem is best tackled using an 'inverse' method, and analysing galaxy-galaxy lensing using maximum likelihood techniques is an example of such a method that we briefly expose below.

Once we have an image catalogue, we process it through a numerical code that retrieves the input parameters of the lenses using a maximum likelihood method as proposed by Schneider & Rix, 1998<sup>33</sup>. For each image ( $i$ ), given a mass model for the foreground lenses galaxies (*e.g.*  $\sigma_0$ ,  $r$ ), we can evaluate the amplification matrix  $a_i$  as a contribution of all the foreground galaxies  $j$  ;  $z_j < z_i$  that lies within a circle of inner radius  $R_{\min}$ , and outer radius  $R_{\max}$  and of centre the position of the image ( $i$ ):

$$a_i(\sigma_0, r) = \sum_{\substack{z_j < z_i \\ d(i, j) < R_{\max}}} a_{ij}(\sigma_0, r) \quad (3)$$

Given the observed ellipticity  $\vec{\varepsilon}_{\text{obs}}^i$  and the associated amplification matrix  $a_i$ , we are able to retrieve the intrinsic ellipticity  $\vec{\varepsilon}_i^s$  of the source before lensing:  $\vec{\varepsilon}_i^s = F(\vec{\varepsilon}_{\text{obs}}^i, a_i(\sigma_0, r)) = \vec{\varepsilon}_i^s(\sigma_0, r)$ . In order to assign a likelihood to the parameters used to describe the lenses galaxies, we use  $P^s$ , the ellipticity probability distribution in the absence of lensing (a Gaussian of width 0.2). Doing that for each image of the catalogue, we construct the likelihood function:  $\mathcal{L}(\sigma_0, r) = \prod_i P^s(\vec{\varepsilon}_i^s)$  which is a function of the parameters used to define the mass model of the lenses. For each pair of parameters, we can compute a likelihood. The larger this function, the more likely the parameters used to describe the lenses.

<sup>a</sup><http://www.oamp.fr/cosmology/lenstool>

## 2.4 Results

We present the results obtained for the simulated data set, for the PIEMD and NFW models in Fig. 2. The point marks the value of the INPUT parameters used in order to generate the simulated catalogue, and the cross stands for the value of the OUTPUT parameters as estimated from the maximum likelihood analysis. Contours represent the  $3\sigma$ ,  $4\sigma$ ,  $5\sigma$  confidence levels, and along the dotted lines, the mass within a projected radius  $R_{\text{aper}} = 100$  kpc is constant, equal to the value indicated on the plot. The conclusion of this theoretical analysis is that we are able to retrieve the INPUT parameters used in order to generate the simulated catalogue, and that the aperture mass is constrained accurately.

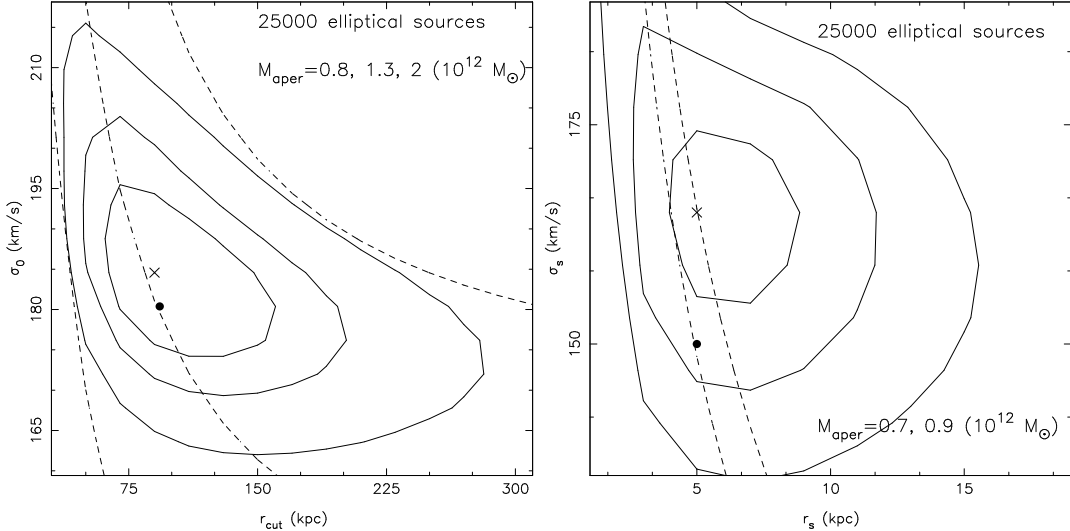


Figure 2: Results of the maximum likelihood analysis on simulated data set: left, using a PIEMD profile; right, using a NFW profile. The point marks the value of the INPUT parameters used in order to generate the simulated catalogue, and the cross stands for the value of the OUTPUT parameters as estimated from the maximum likelihood analysis

## 3 Application to a sample of cluster lenses at $z \sim 0.2$

Given an extensive simulation work described in Paper I, we were confident to apply this maximum likelihood analysis to a sample of massive cluster lenses at  $z \sim 0.2$ , with the aim to constrain the properties of dark matter halos of galaxies living in such a high density environment.

### 3.1 Data and cataloguing

The data were taken at the CFHT with the CFH12K camera through the B, R and I filters. A detailed description of the data acquisition and reduction can be found in Czoske, 2002<sup>11</sup>. The object detection is described in Bardeau et al., 2005<sup>2</sup>. Basic procedures have been implemented, using SEXTRACTOR<sup>5</sup> for object detection and magnitude computations, and the IM2SHAPE software developed by Bridle et al., 2001<sup>8</sup> for PSF subtraction and shape parameters measurements. A master catalogue is produced which matches the objects detected in the three filters and which contains colour indices built from aperture magnitudes. This catalogue is used to plot the colour-magnitude diagrams from which the sequence of elliptical is identified and extracted. These elliptical cluster galaxies are the lenses for the background population. We used only objects detected in all three bands and with reliable shape information, and we undertook a photometric study to derive a redshift estimation for each background galaxy.

### 3.2 Bayesian photometric redshift

We used the HYPERZ<sup>6</sup> software to derive photometric redshifts. Getting photometric redshifts with three bands is quite challenging but possible and reliable for certain redshift ranges which are well constrained by the filters we have. Adding a prior probability allows to get better constraints than we would have without any assumptions. The method implemented here has been developed by Benitez et al, 1999<sup>4</sup>. The idea is to add a prior probability which is not used by HYPERZ and in which we are confident. We will use as a prior the luminosity function of a given galaxy. The final redshift assigned to a galaxy is determined by combining the information coming from the HYPERZ probability distribution with the prior probability distribution. Basically, adding this prior allows us to get rid of some degeneracies in the redshift probability distribution coming from HYPERZ due to using only three filters. From a theoretical analysis (see Paper II for details), we found that our filters are well suited to constrain redshifts from  $z \sim 0.5$  to  $z \sim 1.5$ , i.e. for the background population. On the other hand, redshifts below 0.5 are not well constrained by our filters.

To verify the reliability of the Bayesian photometric redshift estimation, we compare with the DEEP2 redshift survey (Coil et al., 2004<sup>10</sup>): they propose a simple colour-cut designed to select galaxies at  $z > 0.7$ . As discussed in Davis et al., 2005<sup>12</sup>, this colour-cut has proven effective. We check to see where our objects with  $z_{\text{bayes}} > 0.7$  and  $z_{\text{bayes}} < 0.7$  fall in a colour-colour diagram, with respect to this colour-cut. Figure 3 shows the results. The dashed line represents the colour-cut: objects at  $z > 0.7$  are supposed to be above the regions defined by these three dashed lines according to the DEEP2 colour-cut. The points represent our objects for which we have estimated  $z_{\text{bayes}} < 0.7$ . The crosses represent our objects for which we have estimated  $z_{\text{bayes}} > 0.7$ . We can see from this plot that our estimation of the redshift agrees well with the colour-cut.

### 3.3 Results

We applied the maximum likelihood method to the image catalogues. Lenses were extracted from the colour magnitude diagram, and objects with redshift spanning from  $z \sim 0.5$  to  $z \sim 1.5$  were used as the background population. The smooth component corresponding to the cluster itself was also considered; we put a large clump with some parameters derived from a weak lensing analysis by Bardeau et al., 2006<sup>3</sup>. Table 1 summarises the results we obtained using the two different profiles to fit the deformations, and Fig. 3 shows our results (in black) with other results on cluster galaxies (in grey), in the  $(\sigma_0, r_{\text{cut}})$  plane.

The main results are the following: (i) we fit reasonable values for the velocity dispersion, around  $200 \text{ km s}^{-1}$ . This is reasonable in the sense that it is comparable to values inferred using more traditional methods (rotation curves, X ray observations, satellite dynamics) (ii) we find dark matter halos to be very compact compared to field galaxies of equivalent luminosity: considering all cluster galaxies halos, an upper limit on the truncation radius is set at 50 kpc (PIEMD results on Abell 383), when the truncation radius inferred on field galaxies is found to be larger than a few hundreds of kpc (see Fig. 1). The truncation radius is related to the extension of the halo. We can say that cluster galaxies are more compact than field galaxies because the slope of their mass profile steepens earlier, thus the corresponding mass profile reaches a low density value earlier. As a consequence, dark matter halo of cluster galaxies are found to be less extended than they are in the case of field galaxies. The detection with an NFW profile also points out a small spatial extent for the halos: the characteristic radius  $r_s$  is found to be smaller than a few kpc, which corresponds to a concentration parameter  $c > 20$  in agreement with numerical simulations from Bullock et al., 2001<sup>9</sup>.

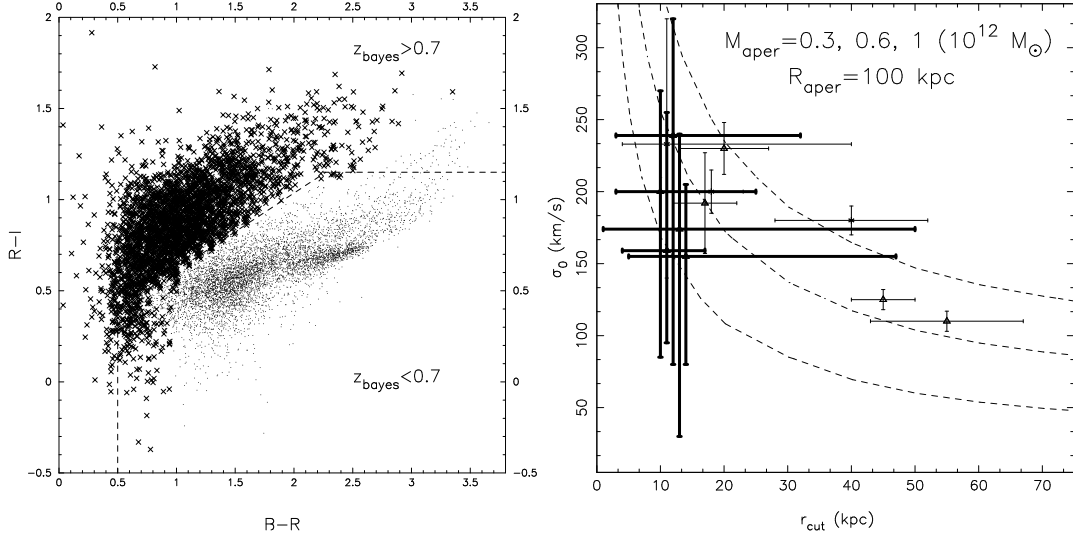


Figure 3: Left: Objects of our Abell 1763 catalogue with  $z_{\text{bayes}} > 0.7$  (crosses) and with  $z_{\text{bayes}} < 0.7$  (dots). The line represents the simple colour-cut used in the DEEP2 survey to select objects with  $z > 0.7$  and  $z < 0.7$ . Right: comparison of our results (black) with the results from Natarajan et al. and Geiger & Schneider (grey)

Cluster	$\sigma_0^*$ , $\text{km s}^{-1}$ (PIEMD)	$r_{\text{cut}}^*$ , kpc (PIEMD)	$r_s^*$ , kpc (NFW)	(M/L)*
A1763	$200^{+70}_{-115}$ ( $3\sigma$ )	$\leq 25$ ( $3\sigma$ )	$\leq 2.5$ ( $3\sigma$ )	$19^{+16}_{-6}$ ( $3\sigma$ )
A1835	$240^{+81}_{-159}$ ( $2\sigma$ )	$\leq 32$ ( $2\sigma$ )	$\leq 5$ ( $2\sigma$ )	$20^{+18}_{-6}$ ( $3\sigma$ )
A2218	$200^{+96}_{-64}$ ( $1\sigma$ )	$\leq 18$ ( $1\sigma$ )	$\leq 1$ ( $1\sigma$ )	$13^{+10}_{-12}$ ( $2\sigma$ )
A383	$175^{+66}_{-143}$ ( $2\sigma$ )	$\leq 50$ ( $2\sigma$ )	$\leq 2.2$ ( $2\sigma$ )	$20^{+13}_{-10}$ ( $3\sigma$ )
A2390	$155^{+50}_{-75}$ ( $1\sigma$ )	$\leq 47$ ( $1\sigma$ )	$\leq 7$ ( $1\sigma$ )	$10^{+21}_{-4}$ ( $1\sigma$ )

Table 1: Summary of the detections, for a  $L^*$  luminosity. The mass corresponds to the total mass computed with a PIEMD profile. Here  $\sigma$  corresponds to the confidence level of the detection

## 4 Conclusion

We have given a revue of galaxy-galaxy lensing detections obtained so far, both on field galaxies as well as on cluster galaxies. We have presented a maximum-likelihood analysis of galaxy-galaxy lensing on simulated data to study the accuracy with which input parameters for mass distributions for galaxies can be extracted.. We have applied this method on a sample of massive galaxy clusters and we have derived some constraints on the dark matter halos of the elliptical cluster galaxies. It is the first time that cluster galaxies are successfully probed from ground based observations. The main result of this work is to find galaxy halos in clusters to be significantly less massive and more compact compared to galaxy halos around field galaxies of equivalent luminosity. This is in good agreement with previous galaxy-galaxy lensing studies. Moreover, this confirmation is based on the analysis of 5 massive clusters lenses whose properties are close one to each other, hence the confirmation we provide is a strong one since it relies on a homogeneous sample.

This observational result is in good agreement with numerical simulations, in particular with the tidal stripping scenario. The theoretical expectation is that the global tidal field of a massive,

dense cluster potential well should be strong enough to truncate the dark matter halos of galaxies that traverse the cluster core (Avila-Reese et al., 2005<sup>1</sup>; Ghigna et al., 2000<sup>17</sup>; Bullock et al., 2001<sup>9</sup>).

## Acknowledgments

Dark Cosmology Centre is funded by the Danish National Research Foundation. PN acknowledges support from NASA via HST grant HST-GO-09722.06-A. ML acknowledges Laurence Tresse and Sophie Maurogordato for organising this meeting.

## References

1. Avila-Reese V. et al., 2005, *ApJ*, 634, 51
2. Bardeau S., Kneib J. P., Czoske O. et al., *A&A*, 434, 433
3. Bardeau S., et al., in prep.
4. Benitez, N., 1999, in ASP Conference Series, Vol. 191, astro-ph/9811189
5. Bertin E. & Arnouts S. 1996, *A&AS*, 117, 393
6. Bolzonella M., Miralles J. M. & Pelló R., 2000, *A&AS*, 363, 476
7. Brainerd T. G., Blandford R. D. & Smail I., 1996, *ApJ*, 466, 623
8. Bridle S., Gull S., Bardeau S., & Kneib J. P. 2001, in Proceedings of the Yale Cosmology Workshop: “The Shapes of Galaxies and their Dark Halos”, ed. N. P. (World Scientific)
9. Bullock J.S. et al., 2001, *MNRAS*, 321, 559
10. Coil A.L. et al., 2004, *ApJ*, 609, 525
11. Czoske O., 2002, PhD thesis, Université Toulouse III – Paul Sabatier
12. Davis M. et al., 2003, *Proc. SPIE*, 4834, 161
13. Dell’Antonio I. P. & Tyson J. A., 1996, *ApJ*, 473, L17
14. Ebbels, T. 1998, PhD thesis, University of Cambridge
15. Fisher P. et al. (the SDSS collaboration), 2000, *ApJ*, 120, 1198
16. Geiger B. & Schneider P., 1999, *MNRAS*, 302, 118
17. Ghigna S., Moore B., Governato F., Quinn T. & Stadel J., 2000, *ApJ*, 544, 616
18. Griffiths R. E., Casertano S., Im M. & Ratnatunga, K.U., 1996, *MNRAS*, 282, 1159
19. Hoekstra H., Franx M., Kuijken K et al., 2003, *MNRAS*, 340, 609
20. Hoekstra H., Yee H. K. C. & Gladders M. D., 2004, *ApJ*, 606, 67
21. Hudson M. J., Gwyn S. D. J., Dahle H. & Kaiser N., 1998, *ApJ*, 503, 531
22. Jaunsen, A.O. 2000, PhD thesis, University of Oslo
23. Kassiola A. & Kovner I., 1993, *ApJ*, 417, 450
24. Kleinheinrich M., 2003, PhD thesis, Bonn University
25. Limousin M., Kneib J.-P. & Natarajan P., 2005, *MNRAS*, 356, 309
26. Limousin M., Kneib J.-P. et al., 2006, submitted to *A&A*
27. Mc Kay, T. A. et al., 2001, submitted to *ApJ*, astro-ph/0108013
28. Natarajan P., Kneib J.-P. Smail I. & Ellis R., 1998, *ApJ*, 499, 600
29. Natarajan P., Loeb A., Kneib J.-P., & Smail I., 2002a, *ApJ*, 580, L17
30. Natarajan P., Kneib J. P. & Smail I., 2002b, *ApJ*, 580, L11
31. Navarro J. F., Frenk C. S., & White S. D. M. 1997, *ApJ*, 462, 563
32. Prada F., Vitvitska M., Klypin A. et al., 2003 *ApJ*, 598, 260
33. Schneider P. & Rix H. W., 1997 *ApJ*, 474, 25
34. Smith D., Bernstein G. M., Fisher P., Jarvis M., 2001 *ApJ*, 551, 643
35. Wilson G., Kaiser N., Luppino G. & Cowie L. L., 2001, *ApJ*, 555, 572